JPET Fast Forward. Published on January 23, 2004 as DOI:10.1124/jpet.103.061986

Role of Adenosine A_{2A} Receptor in the Regulation of Gastric Somatostatin Release

Linda Yip and Yin Nam Kwok

Department of Physiology, University of British Columbia, 2146 Health Sciences Mall,

Vancouver, BC, Canada. V6T 1Z3

Running Title: Adenosine A_{2A} receptors on Somatostatin Release

Corresponding Author: Yin Nam Kwok Ph.D., Department of Physiology, University of British Columbia, 2146 Health Sciences Mall, Vancouver, BC. Canada. V6T 1Z3. Tel: 604-822-6228, Fax: 604-822-6048, email: kynkwok@interchange.ubc.ca

Number of pages text: 38; Number of tables: 0; Number of figures: 10; Number of references: 39; Number of words (Abstract 232; Introduction 673; Discussion 1412)

Non-standard abbreviations used in paper: 2-chloroadenosine (2-CA), N^6-cyclopentyladenosine(CPA), 2-p-(2-carboxyethyl)phenethylamino-5'N-ethylcarboxamidoadenosine (CGS 21680), 5'-N^6-cyclohexyladenosine (CHA), N-ethylcarboxamidoadenosine (NECA), 1-deoxy-1-[6-[[(3-iodophenyl)methyl]amino]-9H-purin-9-yl]-N-methyl-ß-D-ribofuranuronamide (IB-MECA), R(-)-N^6-(2-phenylisopropyl)adenosine (R-PIA), (S)-N^6-(2-phenylisopropyl)adenosine (S-PIA), erythro-9-(2-Hydroxy-3-nonyl)adenine hydrochloride (EHNA), 8-Cyclopentyl-1,3-dipropylxanthine (DPCPX), 4-(2-[7-Amino-2-(2-furyl)[1,2,4]triazolo[2,3-a][1,3,5]triazin-5-ylamino]ethyl)phenol (ZM 241385), somatostatin-like immunoreactivity (SLI), reverse transcriptase polymerase chain reaction (RT-PCR), bovine serum albumin (BSA), Radioimmunoassay (RIA), melting temperatures (Tm), 6-carboxyfluorescein (FAM), 6-carboxytetramethylrhodamine (TAMRA), uracil-N-glycosylase (UNG), normalized reporter emissions (Rn), threshold cycle (C_T), protein gene product 9.5 (PGP 9.5), von Willebrand's factor (VWF), A_{2A} receptor-immunoreacativity (A_{2A}R-IR), immunoreactivity (IR), and phosphate buffered saline (PBS).

Recommended section assignment: Gastrointestinal, hepatic, pulmonary & renal

Abstract

Adenosine has been demonstrated to inhibit gastric acid secretion. In the rat stomach, this inhibitory effect may be mediated indirectly by increasing the release of somatostatin-like immunoreactivity (SLI). Results show that adenosine analogs augmented SLI release in the isolated vascularly perfused rat stomach. The rank order of potency of the analogs in stimulating SLI release was 2-p-(2-carboxyethyl)phenethylamino-5'-N-ethylcarboxamidoadenosine (CGS 21680) ≈ 5'-N-ethylcarboxamidoadenosine > 2-chloroadenosine > R(-)-N^6-(2-phenylisopropyl)adenosine > 1-deoxy-1-[6-[[(3-iodophenyl)methyl]amino]-9H-purin-9-yl]-N-methyl-ß-D-ribofuranuronamide > N^6-cyclopentyladenosine ≈ N^6-cyclohexyladenosine > S(+)-N^6-(2-phenylisopropyl)adenosine, suggesting the involvement of the A_{2A} receptor. In agreement, 4-(2-[7-Amino-2-(2-furyl)[1,2,4]triazolo[2,3-a][1,3,5]triazin-5-ylamino]ethyl)phenol (ZM 241385), an A_{2A} receptor antagonist, was shown to abolish the adenosine- and CGS 21680-stiumlated SLI release. Immunohistochemical studies revealed the presence of A_{2A} receptor immunoreactivity (A_{2A}R-IR) on the gastric plexi and mucosal D-cells, but not on parietal cells and G-cells, suggesting that adenosine may act directly on D-cells or indirectly on the gastric plexi to augment SLI release. The present study also demonstrates that the structure of the mucosal A_{2A} receptor is identical to that in the rat brain, and that alternative splicing of this gene does not occur. A Real-Time RT-PCR assay has also been established to quantify the levels of A_{2A} receptor mRNA. Results show that gastric tissues contained significantly lower levels of A_{2A} receptor mRNA compared to the striatum. The lowest level was detected in the mucosa. In conclusion, adenosine may act on A_{2A} receptors to augment SLI release and consequently control gastric acid secretion.

Adenosine has been demonstrated to modulate a variety of physiological functions by acting on purinergic P1 receptors. These G-protein-coupled receptors are classified into adenosine A_1, A_{2A}, A_{2B}, and A_3 subtypes based on their pharmacological and structural properties. Each subtype has been cloned in the brain tissues of various species including human (Fredholm et al., 2001).

Clinical studies have suggested that changes in the endogenous level of adenosine may influence gastric acid secretion and play a role in ulcer formation. The activity of adenosine deaminase (ADA), a metabolic enzyme of adenosine, appears to be directly correlated with basal and maximal levels of gastric acid output in the fundic mucosa of achlorhydria, gastritis and ulcer patients (Namiot et al., 1990). Patients suffering from hypersecretion of gastric acid were shown to exhibit elevated levels of ADA activity. In gastric ulcer patients, ADA activity in the corpus mucosa was also shown to be reduced following ranitidine treatment (Namiot et al., 1991). These studies, therefore, suggest that adenosine inhibits gastric acid secretion and acts as a gastroprotective agent.

In animal studies, adenosine and its analogs have been shown to protect against gastric ulcers induced by stress (Geiger and Glavin, 1985; Westerberg and Geiger, 1987). This protective effect has been attributed to the inhibitory action of adenosine on acid secretion. Adenosine was shown to suppress gastric acid secretion in several species, including dogs (Gerber et al., 1985; Gerber and Payne, 1988), guinea pigs (Heldsinger et al., 1986), and rats (Glavin et al., 1987; Scarpignato et al., 1987; Westerberg and Geiger, 1989). However, the site of action of adenosine in eliciting this inhibitory response differs among species. Adenosine has been shown to inhibit gastric acid secretion by acting on the acid secreting parietal cells of guinea pigs (Heldsinger et al., 1986) and dogs (Gerber et al., 1985; Gerber and Payne, 1988). In

addition to this direct action, adenosine has also been shown to inhibit the secretion of the acid secretagogue, gastrin, from canine antral G-cells (Schepp et al., 1990). In rats, adenosine analogs did not alter basal or histamine-stimulated aminopyrine uptake in isolated enriched parietal cell preparations (Puurunen et al., 1987). Thus, in this species, adenosine most likely inhibits gastric acid secretion indirectly.

Our laboratory has previously demonstrated that the administration of adenosine to the isolated vascularly perfused rat stomach inhibited immunoreactive gastrin (IR-G) and stimulated somatostatin-like immunoreactivity (SLI) release (Kwok et al., 1990), suggesting that adenosine may regulate gastric acid secretion by modulating gastrin and somatostatin release. Somatostatin, a potent inhibitor of gastric acid secretion, is released from gastric mucosal D-cells (Hersey and Sachs, 1995). Although the stimulatory effect of adenosine on SLI release was shown to be mediated by extracellular adenosine receptors (Kwok et al., 1990), the receptor subtype(s) involved has not been determined. Therefore, the first objective of the present study was to determine the adenosine receptor subtype involved in the stimulatory action of adenosine on SLI release using the isolated vascularly perfused rat stomach and selective adenosine analogs. Preliminary studies suggest that the A_{2A} receptor may be involved. However, the presence of this receptor in functionally distinct regions of the stomach is unknown. The localization of the A_{2A} receptor on specific cells of the stomach, such as the somatostatin-secreting D-cells, is also undetermined. Currently, only the presence of extremely low levels of A_{2A} receptor mRNA has been demonstrated in the whole rat stomach using RT-PCR (Dixon et al., 1996). Therefore, the second objective of this study was to determine the cellular localization, distribution and gene expression levels of the A_{2A} receptor in the rat stomach, using immunohistochemistry, RT-PCR, and Real-Time RT-PCR, respectively. In addition, structural information regarding the gastric

JPET Fast Forward. Published on January 23, 2004 as DOI: 10.1124/jpet.103.061986
This article has not been copyedited and formatted. The final version may differ from this version.

A_{2A} receptor is lacking. The differential expression of multiple A_1 and A_3 receptors transcripts has been demonstrated in different tissues (Fredholm et al., 2001). Since the presence of multiple receptor forms could have important functional implications, the final objective of this study was to determine the cDNA sequence of the rat gastric A_{2A} receptor by cloning and sequencing the entire coding region of the mucosal A_{2A} receptor.

Materials and Methods

Stomach perfusion

Animals were treated in accordance with the guidelines of the University of British Columbia Committee on Animal Care. Male Wistar rats (250 to 325 g) were housed in light and temperature controlled rooms with free access to food and water. Animals were deprived of food for at least 14 h, but had free access to water, prior to stomach perfusion. Rats were anesthetized with i.p. injection (60 mg/kg) of sodium pentobarbital (Somnotol®, MTC Pharmaceuticals, Cambridge, ON, Canada). The surgical procedures used to isolate the stomach for perfusion have previously been described (Kwok et al., 1988; Kwok et al., 1990). Two milliliters saline solution containing 600 U of heparin (Sigma, St. Louis, MO) was introduced into the stomach via this arterial cannula, followed by perfusate. Venous effluent was collected via a portal vein cannula. After a 30 min equilibration period, 5-min samples were collected into ice-cold scintillation vials containing 0.3 ml of Trasylol (aprotinin, 10,000 KIU/ml; Miles Labs., Etobicoke, ON). Aliquots (0.5 ml) were immediately transferred into ice-cold test-tubes containing 0.05 ml Trasylol, and stored at –20°C until assayed.

The stomach was perfused at a rate of 3 ml/min using a peristaltic pump (Cole-Parmer Instrument Co. Chicago, IL). The perfusate was composed of Krebs' solution (in mM: NaCl, 120; KCl, 4.4; $CaCl_2$, 2.5; $MgSO_4 \cdot 7H_2O$, 1.2; KH_2PO_4, 1.5; $NaHCO_3$, 25 and dextrose, 5.1) containing 0.2% BSA (RIA grade; Sigma) and 3% dextran (Clinical grade; Sigma). The perfusate was continuously gassed with a mixture of 95% O_2 and 5% CO_2 to maintain a pH of 7.4. Both the perfusate and the preparation were kept at 37^{o}C by thermostatically controlled heating units throughout the experiment. In some experiments, the perfusion pressure was recorded using a Statham blood pressure transducer (P32 Db), connected at the level of the aortic

cannula, a SE 905 converter and a Gould chart recorder. The perfusion pressure during basal condition was between 52 and 89 mm Hg. The percent (%) change in perfusion pressure was calculated as follows: [recorded pressure during drug perfusion – pressure during basal periods] (mm Hg/2.5 min) ÷ pressure during basal periods (mm Hg/2.5 min) × 100.

Drugs were introduced into the perfusate via side-arm infusion at a rate calculated to give the final perfusion concentrations. The following drugs were purchased from Sigma: adenosine hemisulphate salt, 2-chloroadenosine (2-CA), N^6-cyclopentyladenosine (CPA), 2-p-(2-carboxyethyl)phenethylamino-5'N-ethylcarboxamidoadenosine HCl (CGS 21680), N^6-cyclohexyladenosine (CHA), 5'-N-ethylcarboxamidoadenosine (NECA), R(-)-N^6-(2-phenylisopropyl)adenosine (R-PIA), S(+)-N^6-(2-phenylisopropyl)adenosine (S-PIA), 1-deoxy-1-[6-[[(3-iodophenyl)methyl]amino]-9H-purin-9-yl]-N-methyl-ß-D-ribofuranuronamide (IB-MECA), 8-cyclopentyl-1,3-dipropylxanthine (DPCPX), adenosine deaminase (Type VII; ADA) and sodium nitroprusside. 4-(2-[7-Amino-2-(2-furyl)[1,2,4]triazolo[2,3-a][1,3,5]triazin-5-ylamino]ethyl)phenol (ZM 241385) was procured from Tocris Cookson Inc. (Ellisville, MO). Adenosine analogs were first dissolved in a small volume of DMSO (BDH, Toronto, ON) and subsequently diluted with saline or perfusate to 0.03 or 0.5% before perfusing into the stomach. ADA (100 U/ml) was dialyzed in saline containing 0.2% BSA and the concentration was adjusted according to the final volume before it was diluted with perfusate for perfusion. The perfusion of DMSO alone, at these concentrations, did not alter basal SLI release; the percent change of SLI release in the presence of 0.03 and 0.5% DMSO were –1±2 and –3±3%, respectively.

RIA and data analysis

The specific RIA employed for the measurement of SLI content in samples has previously been described (Kwok et al., 1988; Kwok et al., 1990). The monoclonal antibody, SOMA-3, was used. The drugs used in the present study did not cross-react with this antibody. The inter- and intra-assay variation of the RIA was less than 12 and 8%, respectively.

Although the basal release rate of SLI varied among animals, previous experiments have demonstrated that basal SLI release is well maintained during a 50 min perfusion period (Saffouri et al., 1980; Kwok et al., 1988; Kwok et al., 1990). Therefore, results were expressed as mean ± SEM of SLI release (%), which was calculated as follows: [SLI release (pg/min) during a 5 min period ÷ SLI release (pg/min) during period 1] × 100. To compare the effect of analogs, results were also expressed as percent (%) change (SLI release), which is calculated as follows: [mean SLI release in the presence of drug – mean basal SLI release (periods 1-3)] pg/min ÷ [mean basal SLI release (periods 1-3)] pg/min × 100. Statistical significance ($P < 0.05$) was determined using one-way ANOVA followed by Dunnett's multiple comparison test, and paired or unpaired Student's t-test when appropriate. Statistics and estimation of the EC_{50} were performed using GraphPad Prism (v. 3.0, GraphPad software, San Diego, CA).

Immunohistochemistry

Gastric corpus and antrum tissues from male Wistar rats were fixed overnight, cryoprotected, and sectioned as previously described (Yip et al., 2003). Free-floating sections (30 μm) were sequentially incubated in 0.1 M PBS containing 50 mM NH_4Cl (30 min), 0.1 M PBS containing 100 mM glycine (10 min), and blocking buffer (0.1 M PBS containing 1% BSA and 0.3% Triton X-100, 1 h). Antibodies were diluted in blocking buffer containing 0.1% sodium azide. Sections

were incubated with A_{2A} receptor primary antibody (1:200) for 72 h at 4ºC, washed (0.1 M PBS; 3×15 min), and incubated with cyanine Cy3-conjugated secondary antibody overnight at 4°C. Sections were again washed, and either double stained or mounted onto glass slides. For double staining, tissue sections were incubated with another primary antibody for 72 h at 4°C, washed, and incubated with Alexa Fluor 488-conjugated secondary antibody overnight at 4°C. Sections were then washed, mounted onto glass slides, and coverslipped using a mixture of 0.1 M PBS in glycerin (1:9), and sealed with nail polish.

This rabbit anti-canine A_{2A} receptor antibody (Alpha Diagnostic International, San Antonio, TX) cross-reacts with rat tissues, and has previously been used in this species for immunohistochemistry (Diniz et al., 2003). Its specificity has been established in rat tissues (Nie et al., 1999). In the present study, the specificity of this antibody was confirmed by neutralizing the primary antibody with the control peptide, as suggested by the supplier. Tissues stained with the neutralized antibody did not demonstrate A_{2A} receptor immunoreactivity (A_{2A}R-IR). Additional control experiments were also performed to ensure that non-specific binding did not occur; these included incubating sections with 1% BSA in place of the primary antibody, without the secondary antibody, or with Alexa 488-conjugated anti-mouse IgG secondary antibody. No immunostaining was observed following these procedures. For double staining experiments, monoclonal primary antibodies against somatostatin (1:500; Soma 8, MRC Regulatory peptide group, UBC), gastrin (1:30,000; 109-21 provided by the late Dr. John Walsh), PGP 9.5 (1:200; ab8189, Abcam Limited, Cambridge, UK), human von Willebrand's factor (1:50; Serotec, Oxford, UK) and H^+K^+-ATPase β (1:2000; Affinity Bioreagents Inc., Golden, CO) were used. A_{2A}R-IR was visualized using the secondary antibody, donkey anti-rabbit IgG conjugated to Cy3 (1:2000; Jackson ImmunoResearch, West Grove, PA). All other immunoreactivities were

visualized using donkey anti-mouse IgG conjugated to Alexa Fluor® 488 (1:2000; Molecular Probes, Eugene, OR).

Confocal Microscopy

Tissues were viewed using the Biorad Radiance 2000 confocal scanning laser system mounted on a Nikon Eclipse TE300 inverted microscope. The system uses a krypton gas laser with an excitation wavelength of 568 nm and emission filter 575-625 nm (for visualization of Cy3), and an excitation wavelength of 488 and emission filter 500-530 nm (for visualization of Alexa Fluor 488). Bleed-through was not detected for any of the antibodies used. Lens magnification of ×40 was used with a zoom factor of 1.0 and z-step of 0.5 to 1.0 μm, while lens magnification of ×60 was used with a zoom factor of 1.0-1.6 and a z-step of 0.3 to 0.5 μm. The software program Lasersharp 2000 (v. 4.1, Biorad, Hercules, CA) was used to scan tissues sequentially using the red and green collection channels and the Kalman collection filter (n=2). Images with a resolution of at least 512 × 512 pixels were obtained and then analyzed using NIH image (National Institutes of Health, Bethesda, MD, USA) and Adobe Photoshop (v. 7.0, Adobe systems, San Jose, CA). To determine whether co-localization occurs, the image collected from the red channel (A_{2A}R-IR) was overlaid on the image collected from the green channel (somatostatin, gastrin, VWF, PGP 9.5, or H^+K^+-ATPase β-IR) using Adobe Photoshop.

Quantification of A_{2A}-IR with Somatostatin-IR

Co-localization of A_{2A}R-IR with somatostatin-IR was quantified in the antral and corporeal mucosa by examining at least 3 tissue sections from 4 different animals. For each tissue section, ≥ 4 fields of view, chosen at random, were examined at a magnification of ×40. A total of at

least 55 fields of view were analyzed for quantification in the corpus and antrum. The corporeal and antral mucosa contained 1.1±0.2 and 1.3±0.2 A_{2A}R-IR cells per view, respectively.

RT-PCR

Primer design and synthesis

PCR primers were designed based on previously published rat brain A_{2A} receptor cDNA sequences (Accession number: S47609) (Fink et al., 1992), using the software program PCGene (IntelliGenetics, Mountainview, CA). The forward and reverse primer sequences are 5'CTG CTG AGC CTG CCC AAG TGT3' (corresponding to position 41-61 bp) and 5'CCC TTC TCT TTG GGT TAC CCG3' (corresponding to position 1355-1377 bp), respectively. The amplicon generated (1337 bp) spans the entire coding region of the A_{2A} receptor gene. The primers were synthesized by the Nucleic Acid Protein Services (NAPS) Unit at UBC.

Tissue and total RNA extraction

Male Wistar rats (200-250g) were anaesthetized, and the fundus, corpus, and antrum were dissected out, rinsed in sterile ice-cold saline, and flash frozen in liquid nitrogen. The gastric mucosa was obtained by gently scraping the luminal surface of the stomach using a sterile glass slide. Total RNA was extracted immediately from the mucosa and striatum. The latter tissue has been shown to express high levels of A_{2A} receptor mRNA (Dixon et al., 1996) and was used as a positive control. Total RNA was extracted from tissue using Trizol® reagent (Invitrogen Corp. Carlsbad, CA) according to manufacturer's instructions. The total RNA concentration was determined by the following calculation: concentration (μg/ml) = $A_{260} \times 40$ μg/ml $\times$ 100 (dilution factor).

DNase I treatment, first strand cDNA synthesis and PCR

DNase I treatment was performed at room temperature in 1× first strand buffer [50 mM Tris-HCl (pH 8.3 at 25°C), 75 mM KCl, 3 mM $MgCl_2$] containing 1U DNase I/μg total RNA (Invitrogen), according to manufacturers' instructions. First strand cDNA was synthesized from 5 μg of DNase I-treated total RNA using Superscript II RNase H- Reverse Transcriptase (Invitrogen) according to manufacturers' instructions. As a negative control for RT-PCR, a sample was also prepared using autoclaved distilled water in place of total RNA.

The PCR reaction mixture (50 μl) consisted of 2 μl cDNA in 1× PCR buffer [20 mM Tris-HCl (pH 8.4), and 50 mM KCl] containing 0.2 mM dNTP mix, 4.5 mM $MgCl_2$, 100 ng each of forward and reverse primer, and 1 U Platinum Taq DNA Polymerase (Invitrogen). A positive control sample containing striatal cDNA and a negative control from the first strand synthesis step were included for all experiments. The PCR was performed using the Robocycler Temperature cycler (Stratagene, La Jolla, CA). Thirty cycles of amplification were performed. Each cycle consisted of a 45 sec denaturation period at 94°C, a 1 min annealing period at 58°C, and a 1 min extension period at 72°C. PCR products were separated by gel electrophoresis, visualized and photographed under UV light using the Stratagene Eagle Eye II System.

Cloning and Sequencing of the mucosal A_{2A}R gene

The PCR product generated using mucosa tissue as the template was ligated into the pGEM-T vector (Promega, Madison, WI). DHα-competent E. coli cells (Invitrogen) were transformed with this vector and grown in LB plates containing ampicillin (100 μg/ml), IPTG (0.5 mM), and X-Gal (80 μg/ml). Plasmid DNA was purified using the QIAprep Miniprep kit (Qiagen). Samples were sequenced at the NAPS Unit using the T7 primer, the SP6 primer, and the

following two primers, which were designed based on the rat brain A_{2A} receptor gene (accession #S47609): 5' TTG TCC TGG TCC TCA CGC 3' (position 313-330 bp) and 5' AGG GCC GGG TGA CCT GTC 3' (position 541-558 bp). The gene sequence of the mucosal A_{2A} receptor was aligned with the published sequence in the rat brain using the "University of Southern California (USC) Sequence Alignment Server" (www.hto.usc.edu/software) and submitted to the GenBank database at the National Center for Biotechnology Information.

Quantification of A_{2A}R gene expression by Real-time RT-PCR

A two-step Real-Time RT-PCR assay was performed to quantify A_{2A} receptor gene expression in various regions of the rat stomach. For comparison, A_{2A} receptor gene expression levels were also measured in the rat striatum.

Primers, probes and A_{2A} receptor RNA standards for Real-time PCR

Primers and probes were designed using the Primer Express Sequence Design software program (v. 1.0, Applied Biosystems, Foster City, CA). The reporter dye, 6-carboxyfluorescein (FAM) and the quencher dye, 6-carboxytetramethylrhodamine (TAMRA) were linked to the 5' and 3' ends of the A_{2A} receptor probe, respectively. The sequences of the forward primer, reverse primer, and probe are 5'ACCCCTTCATCTACGCCTACAG3', 5'CGTGGGTTCGGATGATCTTC3', and FAM-5'CGGGAGTTCCGCCAGACCTTCC3'-TAMRA, which correspond to positions 910-931, 978-997 and 939-957 bp of the rat brain A_{2A} receptor gene (accession #S47609), respectively. The primer and probes were synthesized by the NAPS Unit at UBC and by Synthegen, LLC (Houston, TX), respectively.

RNA transcripts expressing the entire coding region of the A_{2A} receptors were used as the standards for quantification during Real-Time RT-PCR. The standards were synthesized using plasmids generated by the previous cloning experiments by *in vitro* transcription using the Riboprobe *in vitro* transcription kit and T7 RNA polymerase (Promega). A_{2A} receptor RNA standards were DNase I-treated, and purified. A_{2A} RNA standard concentrations were determined using the RiboGreen Reagent Quantitation kit (Molecular Probes), the FL600 Microplate Fluorescence reader (Biotek Inc., Winooski, VT), and the KC4 Kineticalc Software (version 2.6, Biotek Inc.), according to manufacturer's instructions. RNA standards were serially diluted to 1×10^3 to 1×10^{12} copies/μl in RNase-free water, aliquoted, stored at –80°C, and thawed only once prior to use.

Two Step Real-Time RT- PCR

A_{2A} receptor gene expression was measured in extracts from the whole fundus, corpus, antrum, the corporeal mucosa and corporeal muscle layers, and the whole stomach mucosa ($n \geq 4$). The methods for tissue extraction were described earlier. To obtain the corporeal mucosa and muscle tissue, the corporeal mucosa was gently scraped off the luminal surface of the corpus using a sterile glass slide. The remaining corporeal muscle tissue was flash frozen in liquid nitrogen. Total RNA was extracted immediately from corporeal and whole stomach mucosa samples. The striatum was also used as a positive control in this experiment. Total RNA was isolated, quantified, and DNase I-treated as previously described.

Step 1: Reverse Transcription

One μg of DNase I-treated tissue RNA was reverse transcribed in a total volume of 10 μl containing 200 ng random hexamers, 20 U RNAguard RNase inhibitor, 1× first strand buffer, 10

mM DTT, 0.5 mM dNTP mix, and 100 U Superscript II RNase H-Reverse Transcriptase. At least 6 concentrations of the A_{2A} receptor RNA standard, ranging from 1×10^3 to 1×10^6 copies/µl, and a sample containing DNase I-treated RNase-free water in place of the template, were reverse transcribed simultaneously. The reverse transcribed RNA standards were used to construct the standard curve for the Real-Time PCR assay, and the sample containing the sterile water was used as the template for the negative control.

Step 2: PCR

Each assay consisted of 6 standard curve samples, a negative control sample, and unknown samples. All reactions were performed in triplicates. The PCR reaction mixture (25 µl) consisted of 1× TaqMan buffer A, 200 µM of each dATP, dCTP, and dGTP, 400 µM dUTP, 0.01 U/µl AmpErase uracil-N-glycosylase (UNG) and 0.025 U/µl AmpliTaq Gold DNA polymerase from the TaqMan PCR Core Kit (Applied Biosystems, Foster City, CA) and also contained 0.5 µl of tissue cDNA, standard cDNA or negative control, 100 nM probe, 100 nM each of the forward and reverse primers, and 4.5 mM $MgCl_2$. The reaction was performed using the ABI Prism 7700 Sequence Detector (Applied Biosystems) with the following cycling parameters: 2 min hold at 50°C for UNG incubation, 10 min hold at 95°C for AmpliTaq Gold activation, followed by 40 cycles of amplification consisting of a 15 s denaturation step at 95°C and 1 min anneal/extend period at 60°C.

Data Collection and Analysis

Data were collected during each PCR cycle, and analyzed using the Sequence Detection Software (v. 1.6.3, Applied Biosystems). An amplification plot showing normalized reporter emissions (Rn) vs. cycle number was generated. The threshold cycle (C_T), the cycle where an

increase in fluorescence is associated with exponential growth, was determined by the software using the fluorescence emitted during the first 15 cycles. A standard curve of C_T vs. Log (initial A_{2A} receptor standard concentrations) was generated (See Fig. 10C). The initial concentration of each unknown sample was determined by interpolation using the C_T value determined by the assay. The correlation coefficient of each standard curve was > 0.95, and the C_T of the no template controls exceeded 40 cycles in every assay, indicating the absence of DNA contamination. Results were expressed as copies of mRNA per μg total RNA. Statistical significance was determined using GraphPad Prism and the two-tailed unpaired Student's t-test, where $P < 0.05$ was considered significant.

JPET Fast Forward. Published on January 23, 2004 as DOI: 10.1124/jpet.103.061986
This article has not been copyedited and formatted. The final version may differ from this version.

Results

Effect of adenosine agonists on gastric SLI release

Various adenosine receptor selective and non-selective analogs were used in the present study to examine the adenosine receptor(s) involved in the regulation of SLI release, since specific agonists for individual receptor subtypes are unavailable. The effect of the A_1 (CHA, CPA, R-PIA and S-PIA), A_{2A} (CGS 21680), A_2 (NECA), and A_3 (IB-MECA) selective, and the non-selective agonists (2-CA) on SLI release was tested and compared. The basal release rate of SLI during periods 1 to 3 was shown to remain relatively constant in experiments examining the effect of 0.1 μM CPA (174±24 to178±27 pg/min), 1 μM CPA (146±20 to 162±19 pg/min), 0.1 μM CGS 21680 (92±18 to 95±18 pg/min) and 0.1 μM IB-MECA (191±39 to 199±47 pg/min) on SLI release (Fig. 1). Figure 1A shows that the administration of 0.1 μM CPA caused a significant inhibition of SLI release. SLI release returned to basal levels 5 min after the cessation of CPA perfusion. However, when 1 μM CPA was perfused into the stomach, the release of SLI was enhanced starting at period 6. The increased release returned to basal levels upon withdrawal of the drug (Fig. 1B). When 0.1 μM CGS 21680 was perfused into the stomach, the increase in SLI release was immediately apparent (Fig. 1C). Upon the cessation of CGS 21680 perfusion, SLI release returned to basal levels within 10 min. The perfusion of IB-MECA also increased SLI release significantly at periods 7 and 8. SLI release returned to basal levels 10 min after the withdrawal of the drug perfusion (Fig. 1D).

To test the concentration dependency of adenosine analogs in stimulating the release of SLI, similar experiments were performed using different concentrations of adenosine analogs. Results are expressed as percent (%) changes in SLI release and are summarized in Fig. 2. These analogs caused concentration-dependent increases in SLI release. CGS 21680 and NECA caused

significant augmentation of SLI release starting at 0.01 μM, and a maximal response was achieved at 1 μM. The EC_{50} of both CGS 21680 and NECA in stimulating SLI release was estimated to be 0.06 μM, with a 95% confidence interval between 0.02 and 0.17 μM, and 0.03 and 0.14 μM, respectively. At higher concentrations (1 and 10 μM), CHA and CPA enhanced SLI release. Although it is not apparent in Fig. 2, lower concentrations of CHA (0.1 μM) and CPA (0.01 and 0.1 μM) significantly ($P < 0.05$) inhibited SLI release (see Fig. 1A). The % changes of SLI release in the presence of 0.1 μM CHA, and 0.01 and 0.1 μM CPA were –16±6, and –12±3 and –19±5%, respectively. The rank order of potency of the analogs in augmenting SLI release was CGS 21680 ≈ NECA > 2-CA > R-PIA > IB-MECA > CPA ≈ CHA > S-PIA.

The effect of CGS 21680 on perfusion pressure was also examined. The administration of CGS 21680 significantly decreased perfusion pressure in a concentration-dependent manner, (Fig. 3). To test if the stimulated SLI release is due to a vasodilatory action, the effect of nitroprusside, a potent vasodilator, on perfusion pressure and SLI release was examined. Nitroprusside (1 μM) also significantly decreased perfusion pressure (Fig. 3), but did not alter gastric SLI release; the % change in SLI release was shown to be 0±2%.

Effect of ZM 241385 and DPCPX on SLI release

The effect of the antagonists, ZM 241385 (A_{2A} selective) and DPCPX (A_1 selective) on basal and agonist-stimulated SLI release were examined. To test the effect of ZM 241385 on CGS 21680-stimulated SLI release, the antagonist was perfused 5 min before the concomitant perfusion of both agonist and antagonist for 15 min. Figure 4A shows that the release of SLI was augmented when 0.1 μM CGS 21680 was introduced into the stomach alone for 15 min. The perfusion of ZM 241385 decreased basal SLI release (Fig. 4B). When ZM 241385 was perfused

concomitantly with CGS 21680, the stimulated release of SLI was abolished (Fig. 4C). For comparison, results are expressed in % change of SLI release and summarized in Fig. 5. Both 1 and 10 μM ZM 241385 suppressed basal SLI release and blocked the effect of 0.1 μM CGS 21680 on SLI release. The % changes of SLI release during the perfusion of both 1 and 10 μM ZM 241385 with 0.1 μM CGS 21680 were similar to the % change in SLI release when the antagonist (1 or 10 μM) was perfused alone. ZM 241385 was also shown to block adenosine (1 μM)-induced SLI release (Fig.5). The % change of SLI release during the perfusion of ZM 241385 together with adenosine (–51±1%) is lower than that of the antagonist alone (–38±10%). The effect of 1 μM DPCPX on basal and 0.1 μM CGS 21680-induced SLI release was also tested. DPCPX inhibited basal SLI release (Fig. 5). However, the CGS 21680-induced SLI release was not altered in the presence of DPCPX.

Involvement of endogenous adenosine in SLI release

The effect of ADA and EHNA, an ADA inhibitor, on SLI release was examined. Drugs were perfused into the stomach for 20 min after a 15 min basal period. Results are summarized in Fig. 6. EHNA and ADA caused a concentration-dependent increase and decrease in basal SLI release, respectively (Fig. 6A). Adenosine-induced SLI release was also enhanced and inhibited by the presence of EHNA and ADA, respectively (Fig. 6B).

Cellular localization and distribution of A_{2A}R-IR

The perfusion studies suggest that the A_{2A} receptor is involved in the augmentation of SLI release. Therefore, experiments were performed to examine the cellular localization and distribution of A_{2A} receptors in the rat stomach. Results show that the distribution of A_{2A}R-IR

was similar in the corpus and antrum. In both regions, intense A_{2A} receptor staining was observed on mucosal cells, cell bodies and nerve fibers of the myenteric plexus, and nerve fibers of the circular muscle layer, longitudinal muscle layer, muscularis mucosae and submucosal plexus (Fig. 7). A_{2A}R-IR was also observed on blood vessels of both the corpus and antrum.

Double-staining for A_{2A}R-IR and somatostatin-IR was performed to examine whether A_{2A} receptors are expressed on somatostatin-secreting D-cells of the mucosa. Somatostatin-IR was abundant in the mucosa, but sparse in other layers of the stomach. Co-localization of A_{2A}R-IR with somatostatin-IR was frequently observed on cells of both the corporeal (Fig. 8 A-C) and antral mucosa (Fig. 8 D-F). Quantification of this co-localization demonstrated that 33±4% and 32±8% of A_{2A}R-IR cells also expressed somatostatin-IR in the corporeal and antral mucosa, respectively. In rare occasions, A_{2A}R-IR was also shown to co-localize with somatostatin-IR in the myenteric plexus of the corpus (Fig. 8 G-I) and antrum (Fig. 8 J-L).

Double staining experiments were also performed to localize A_{2A}R-IR in relation to the immunoreactivity (IR) of gastrin, H^+K^+-ATPase β (parietal cell marker), VWF (endothelial cell marker), and PGP 9.5 (neuronal marker). Results show that A_{2A}R-IR was not co-localized with H^+K^+-ATPase β-IR (Fig. 9 A-C) or gastrin-IR (Fig. 9 D-F). However, extensive co-localization of VWF-IR with A_{2A}R-IR was observed in the muscle layers, myenteric and submucosal plexi (Fig. 9 G-I). In both the corpus and antrum, A_{2A}R-IR was shown to be co-localized with PGP 9.5-IR in cell bodies and nerve fibers of the myenteric plexus, nerve fibers of the submucosal plexus, circular and longitudinal muscle layers, and muscularis mucosae (Fig. 9 J-L).

Regional Distribution, Structure, and Abundance of Adenosine A_{2A} Receptor mRNA

RT-PCR demonstrated the presence of A_{2A} receptor mRNA in all gastric regions examined, including the fundus, corpus, antrum, and mucosa. Abundant A_{2A} receptor mRNA was also detected in the rat striatum, which was used as a positive control (Fig. 10 A). For each tissue, only one RT-PCR amplicon was generated. In addition, cloning and sequencing results demonstrated that the coding region of the gastric mucosal A_{2A} receptor (submitted to GenBank; accession number: AF228684) was identical to the published sequence in the rat brain (Fink et al., 1992) (accession number: S47609).

Results also show that A_{2A} receptor gene expression levels did not differ significantly among the fundus, corpus, and antrum. The mRNA level of the A_{2A} receptor was lower in the whole stomach mucosa and corporeal mucosa than in the whole fundus, corpus, and antrum (Fig. 10B). The A_{2A} receptor mRNA levels in gastric tissues were significantly lower in comparison to the striatum. The striatum contained 2.2×10^6 copies of A_{2A} receptor mRNA/μg total RNA, which was at least 70× higher than in any region of the stomach. The standard curve generated by the A_{2A} receptor Real-Time PCR assay was able to measure a 7 log range of concentrations (Fig. 10C). Thus, striatal and gastric A_{2A} receptor gene expression levels were quantified simultaneously in the same assay.

Discussion

Studies have shown that adenosine may play a role in regulating gastric acid secretion and protecting the stomach against ulceration. In the rat, adenosine has not been shown to act directly on parietal cells, and our laboratory has suggested that adenosine may exert its inhibitory effect on acid secretion by releasing somatostatin (Kwok et al., 1990). Results of the present experiments demonstrate that adenosine-induced SLI release is likely mediated by activation of the adenosine A_{2A} receptors. This was suggested by the following rank order of potency of adenosine analogs in augmenting SLI release: CGS 21680 ≈ NECA > 2-CA > R-PIA > IB-MECA > CPA ≈ CHA > S-PIA. CGS 21680 is a potent A_{2A} receptor agonist which exhibits a 140-fold selectivity for A_{2A} receptors over A_1 receptors (Hutchison et al., 1989). Results shows that the stimulatory effect of CGS 21680 (1 and 10 μM) on SLI release (% increase) was at least 6-fold greater than that elicited by similar concentrations of CPA or CHA. Although CPA and CHA were able to stimulate basal SLI release, it is conceivable that at these high concentrations they were acting non-specifically on A_{2A} rather than A_1 receptors. The lack of an effect of DPCPX (1 μM) on CGS 21680-induced SLI release also suggests that A_1 receptors are not involved. This concentration of DPCPX has been shown to completely abolish A_1 receptor mediated response (Lohse et al., 1987). The stimulatory effect of CGS 21680 is unlikely mediated by A_{2B} receptors since this compound has a much lower affinity for the A_{2B} receptor (Brackett and Daly, 1994). Although CGS 21680 and NECA stimulated gastric SLI release equipotently and with similar efficacy, the calculated EC_{50} for both compounds were in the sub-micromolar range (0.06 μM) rather than the micromolar range, as suggested for A_{2B} receptors (Brackett and Daly, 1994; Klotz et al., 1998). In addition, the stimulatory effect of CGS 21680 and adenosine was completely blocked by the A_{2A} selective antagonist, ZM 241385 (Poucher et

al., 1995). Although the A_3 selective agonist, IB-MECA (Gallo-Rodriguez et al., 1994), also enhanced SLI release, the effect was about 7-fold less than CGS 21680. In rats, A_3 receptor mediated effects were shown to be resistant to 8-phenyltheophylline (8-PT) blockade (van Galen et al., 1994; Peachey et al., 1996). The observation that 8-PT can abolish adenosine-induced SLI release (Kwok et al., 1990) supports the lack of A_3 receptor involvement. The possibility that the adenosine A_{2A} receptor mediated augmentation of SLI release is secondary to a vasodilatory action may also be ruled out since the vasodilator, nitroprusside, did not alter SLI release.

Results show that the A_1 selective analogs, CPA (0.01 and 0.1 μM) and CHA (0.1 μM) caused a small but significant inhibition of SLI release, suggesting that A_1 receptor activation may exert an inhibitory effect on SLI release. A similar result was obtained with 0.01 μM adenosine (Kwok et al., 1990). This A_1 receptor-mediated inhibitory effect may be a result of the preferential activation of A_1 receptor by low concentrations of adenosine as previously suggested (Ralevic and Burnstock, 1998). Results also show that blockade of A_{2A} receptors by ZM 241385 resulted in significant suppression of basal SLI release. This observation may be due to the unmasking of the inhibitory A_1 receptors. Under this condition, endogenous adenosine may act only on the A_1 receptors. This proposal was also supported by the observation that the inhibition of SLI release caused by the perfusion of both ZM 241385 and adenosine was greater than that caused by the antagonist alone. The stimulatory effect of adenosine, CPA and CHA on SLI release may then be attributed to their abilities to activate A_{2A} receptor at higher concentrations. The effect of DPCPX on A_1 receptor-mediated inhibition of SLI release was not tested since the administration of DPCPX alone also inhibited SLI release. The explanation for the inhibition is, at present, unclear.

Results also shows that EHNA, an ADA inhibitor (Mendelson et al., 1983), increased basal and potentiated adenosine-stimulated SLI release, suggesting that endogenous adenosine is involved in the regulation of SLI release. Similar results were obtained when the adenosine uptake inhibitor, dipyridamole, was used (Kwok et al., 1990). In the canine parietal cell preparation, the addition of ADA enhanced histamine-stimulated aminopyrine uptake (Gerber and Payne, 1988). In the present study, the administration of ADA was shown to decrease basal SLI release. Although the present study did not examine the effectiveness of the various doses of ADA on endogenous adenosine metabolism, ADA was shown to suppress the effect of exogenous administered adenosine. Therefore, an increase or decrease in the availability of adenosine may alter SLI release leading to changes in gastric acid secretion.

Results of the present experiments also demonstrate that the sequence of the coding region of the gastric mucosal A_{2A} receptor was identical to that in the rat brain (Fink et al., 1992). Since multiple transcripts of the A_{2A} receptor were not detected in the PCR experiments, alternative splicing of this receptor is unlikely to occur in the rat stomach. The present experiments demonstrate that this A_{2A} receptor gene was expressed in several functionally and morphologically distinct regions of the stomach, including the fundus, corpus, antrum and mucosa. The A_{2A} receptor mRNA levels in these tissues were quantified using Real-Time RT-PCR. This assay was able to measure as little as 5×10^2 copies of A_{2A} receptor RNA/μg total tissue RNA and over a 7 log range of concentrations. Results demonstrate that the lowest level of A_{2A} receptor mRNA level was present in the gastric mucosa and the level in the striatum was at least 70 fold higher than any gastric regions. These results correspond well with results obtained from the immunohistochemistry studies. Although intense and distinct A_{2A}R-IR was

present on some mucosal cells, the majority of A_{2A}R-IR was observed on nerve fibers and vasculature of the muscle layers and the myenteric plexus.

The present study shows that somatostatin-IR resided in the D-cells, as previously reported (Ekblad et al., 1985; Keast et al., 1985). Sparse staining for this peptide was observed in the myenteric plexus and on nerve fibers of the circular muscle. These fibers appears not to project to the mucosa. The present study shows that A_{2A}R-IR was present on mucosal D-cells. Although A_{2A}R-IR also co-localized with somatostatin-IR in the myenteric plexus, this occurrence was rare. Thus, it is likely that adenosine and its analogs act directly on mucosal D-cells to elicit SLI release. Increases in gastrin and gastric acid secretion have been shown to stimulate SLI release (Hersey and Sachs, 1995). The lack of co-localization of A_{2A}R-IR with gastrin-IR or H^+K^+-ATPase β suggests that the effect of adenosine on SLI release is not mediated indirectly by its action on G-cells or parietal cells.

In addition to somatostatin-IR, A_{2A}R-IR was also co-localized with VWF-IR throughout the corpus and antrum. This observation agrees well with the known vascular action of adenosine (Tabrizchi and Bedi, 2001) and with the results of the present perfusion pressure study. The localization of A_{2A} receptors in the nerve fibers of the myenteric and submucosal plexus is not surprising since previous studies have demonstrated their presence in the enteric plexi. A_{2A} receptors have been shown to be expressed on myenteric and submucosal neurons of the jejunum and colon (Christofi et al., 2001), and are involved in the modulation of enteric neural transmission (Barajas-Lopez et al., 1991). Activation of neuronal A_{2A} receptors has also been shown to modulate noradrenaline and acetylcholine mediated neural transmission (Sebastiao and Ribeiro, 1996). Although the gastric release of SLI is regulated by these neurotransmitters (Saffouri et al., 1980; Koop et al., 1983), it is unlikely that adenosine modulates SLI release

through A_{2A} receptor-mediated changes in acetylcholine and noradrenaline release. We have previously shown that the cholinergic blockers, atropine and hexamethonium, and the β-adrenergic blocker, propranolol, did not alter adenosine-induced changes in SLI release (Kwok et al., 1990). However, the possibility that adenosine stimulates SLI release indirectly by modulating non-cholinergic and non-adrenergic neural transmission cannot be ruled out.

In conclusion, the present study demonstrates that the brain and gastric mucosal A_{2A} receptor are structurally identical. A sensitive Real-Time RT-PCR method has been established to quantify adenosine A_{2A} receptor gene expression. Stimulation of gastric A_{2A} receptors enhances the release of SLI and may subsequently inhibit gastric acid secretion. Adenosine is likely to exert this effect, at least in part, by acting directly on A_{2A} receptors of gastric D-cells. This suggestion is supported by immunohistochemistry studies showing the co-localization A_{2A}R-IR with somatostatin-IR on D-cells.

Acknowledgements

The authors wish to thank Henry Chi Hang Leung for his excellent technical assistance.

References

Barajas-Lopez C, Surprenant A and North RA (1991) Adenosine A1 and A2 receptors mediate presynaptic inhibition and postsynaptic excitation in guinea pig submucosal neurons. *J Pharmacol Exp Ther* 258:490-495.

Brackett LE and Daly JW (1994) Functional characterization of the A2b adenosine receptor in NIH 3T3 fibroblasts. *Biochem Pharmacol* 47:801-814.

Christofi FL, Zhang H, Yu JG, Guzman J, Xue J, Kim M, Wang YZ and Cooke HJ (2001) Differential gene expression of adenosine A1, A2a, A2b, and A3 receptors in the human enteric nervous system. *J Comp Neurol* 439:46-64.

Diniz C, Leal S and Goncalves J (2003) Regional differences in the adenosine A(2) receptor-mediated modulation of contractions in rat vas deferens. *Eur J Pharmacol* 460:191-199.

Dixon AK, Gubitz AK, Sirinathsinghji DJ, Richardson PJ and Freeman TC (1996) Tissue distribution of adenosine receptor mRNAs in the rat. *Br J Pharmacol* 118:1461-1468.

Ekblad E, Ekelund M, Graffner H, Hakanson R and Sundler F (1985) Peptide-containing nerve fibers in the stomach wall of rat and mouse. *Gastroenterology* 89:73-85.

Fink JS, Weaver DR, Rivkees SA, Peterfreund RA, Pollack AE, Adler EM and Reppert SM (1992) Molecular cloning of the rat A2 adenosine receptor: selective co-expression with D2 dopamine receptors in rat striatum. *Brain Res Mol Brain Res* 14:186-195.

Fredholm BB, AP IJ, Jacobson KA, Klotz KN and Linden J (2001) International Union of Pharmacology. XXV. Nomenclature and classification of adenosine receptors. *Pharmacol Rev* 53:527-552.

Gallo-Rodriguez C, Ji XD, Melman N, Siegman BD, Sanders LH, Orlina J, Fischer B, Pu Q, Olah ME, van Galen PJ and et al. (1994) Structure-activity relationships of N6-

benzyladenosine-5'-uronamides as A3-selective adenosine agonists. *J Med Chem* 37:636-646.

Geiger JD and Glavin GB (1985) Adenosine receptor activation in brain reduces stress-induced ulcer formation. *Eur J Pharmacol* 115:185-190.

Gerber JG, Nies AS and Payne NA (1985) Adenosine receptors on canine parietal cells modulate gastric acid secretion to histamine. *J Pharmacol Exp Ther* 233:623-627.

Gerber JG and Payne NA (1988) Endogenous adenosine modulates gastric acid secretion to histamine in canine parietal cells. *J Pharmacol Exp Ther* 244:190-194.

Glavin GB, Westerberg VS and Geiger JD (1987) Modulation of gastric acid secretion by adenosine in conscious rats. *Can J Physiol Pharmacol* 65:1182-1185.

Heldsinger AA, Vinik AI and Fox IH (1986) Inhibition of guinea-pig oxyntic cell function by adenosine and prostaglandins. *J Pharmacol Exp Ther* 237:351-356.

Hersey SJ and Sachs G (1995) Gastric acid secretion. *Physiol Rev* 75:155-189.

Hutchison AJ, Webb RL, Oei HH, Ghai GR, Zimmerman MB and Williams M (1989) CGS 21680C, an A2 selective adenosine receptor agonist with preferential hypotensive activity. *J Pharmacol Exp Ther* 251:47-55.

Keast JR, Furness JB and Costa M (1985) Distribution of certain peptide-containing nerve fibres and endocrine cells in the gastrointestinal mucosa in five mammalian species. *J Comp Neurol* 236:403-422.

Klotz KN, Hessling J, Hegler J, Owman C, Kull B, Fredholm BB and Lohse MJ (1998) Comparative pharmacology of human adenosine receptor subtypes - characterization of stably transfected receptors in CHO cells. *Naunyn Schmiedebergs Arch Pharmacol* 357:1-9.

Koop H, Behrens I, Bothe E, Koschwitz H, McIntosh CH, Pederson RA, Arnold R and Creutzfeldt W (1983) Adrenergic control of rat gastric somatostatin and gastrin release. *Scand J Gastroenterol* 18:65-71.

Kwok YN, McIntosh C and Brown J (1990) Augmentation of release of gastric somatostatin-like immunoreactivity by adenosine, adenosine triphosphate and their analogs. *J Pharmacol Exp Ther* 255:781-788.

Kwok YN, McIntosh CH, Sy H and Brown JC (1988) Inhibitory actions of tachykinins and neurokinins on release of somatostatin-like immunoreactivity from the isolated perfused rat stomach. *J Pharmacol Exp Ther* 246:726-731.

Lohse MJ, Klotz KN, Lindenborn-Fotinos J, Reddington M, Schwabe U and Olsson RA (1987) 8-Cyclopentyl-1,3-dipropylxanthine (DPCPX)--a selective high affinity antagonist radioligand for A1 adenosine receptors. *Naunyn Schmiedebergs Arch Pharmacol* 336:204-210.

Mendelson WB, Kuruvilla A, Watlington T, Goehl K, Paul SM and Skolnick P (1983) Sedative and electroencephalographic actions of erythro-9-(2-hydroxy-3-nonyl)-adenine (EHNA): relationship to inhibition of brain adenosine deaminase. *Psychopharmacology* 79:126-129.

Namiot Z, Rutkiewicz J, Stasiewicz J, Baranczuk E and Marcinkiewicz M (1991) Adenosine deaminase activity in the gastric mucosa in patients with gastric ulcer. Effects of ranitidine and sucralfate. *Eur J Pharmacol* 205:101-103.

Namiot Z, Rutkiewicz J, Stasiewicz J and Gorski J (1990) Adenosine deaminase activity in the human gastric mucosa in relation to acid secretion. *Digestion* 45:172-175.

Nie Z, Mei Y, Malek RL, Marcuzzi A, Lee NH and Ramkumar V (1999) A role of p75 in NGF-mediated down-regulation of the A(2A) adenosine receptors in PC12 cells. *Mol Pharmacol* 56:947-954.

Peachey JA, Hourani SM and Kitchen I (1996) Differential development of adenosine A1 and A2b receptors in the rat duodenum. *Br J Pharmacol* 119:949-958.

Poucher SM, Keddie JR, Singh P, Stoggall SM, Caulkett PW, Jones G and Coll MG (1995) The in vitro pharmacology of ZM 241385, a potent, non-xanthine A2a selective adenosine receptor antagonist. *Br J Pharmacol* 115:1096-1102.

Puurunen J, Ruoff HJ and Schwabe U (1987) Lack of direct effect of adenosine on the parietal cell function in the rat. *Pharmacol Toxicol* 60:315-317.

Ralevic V and Burnstock G (1998) Receptors for purines and pyrimidines. *Pharmacol Rev* 50:413-492.

Saffouri B, Weir GC, Bitar KN and Makhlouf GM (1980) Gastrin and somatostatin secretion by perfused rat stomach: functional linkage of antral peptides. *Am J Physiol* 238:G495-501.

Scarpignato C, Tramacere R, Zappia L and Del Soldato P (1987) Inhibition of gastric acid secretion by adenosine receptor stimulation in the rat. *Pharmacology* 34:264-268.

Schepp W, Soll AH and Walsh JH (1990) Dual modulation by adenosine of gastrin release from canine G-cells in primary culture. *Am J Physiol* 259:G556-563.

Sebastiao AM and Ribeiro JA (1996) Adenosine A2 receptor-mediated excitatory actions on the nervous system. *Prog Neurobiol* 48:167-189.

Tabrizchi R and Bedi S (2001) Pharmacology of adenosine receptors in the vasculature. *Pharmacol Ther* 91:133-147.

van Galen PJ, van Bergen AH, Gallo-Rodriguez C, Melman N, Olah ME, AP IJ, Stiles GL and Jacobson KA (1994) A binding site model and structure-activity relationships for the rat A3 adenosine receptor. *Mol Pharmacol* 45:1101-1111.

Westerberg VS and Geiger JD (1987) Central effects of adenosine analogs on stress-induced gastric ulcer formation. *Life Sci* 41:2201-2205.

Westerberg VS and Geiger JD (1989) Adenosine analogs inhibit gastric acid secretion. *Eur J Pharmacol* 160:275-281.

Yip L, Kwok YN and Buchan AM (2003) Cellular localization and distribution of neurokinin-1 receptors in the rat stomach. *Auton Neurosci* 104:95-108.

Footnotes:

This work was supported by the Canadian Apoptosis Research Foundation Society, Canada Foundation for Innovation, Wah Sheung Fund and the former BCHRF. Linda Yip was supported by the Cordula and Gunter Paetzold Fellowship and the University of British Columbia Graduate Fellowship.

A portion of this work was included in Linda Yip's Ph.D. thesis entitled: Adenosine A_1 and A_{2A} Receptors in the Rat Stomach: Biological Actions, Cellular Localization, Structure, and Gene Expression.

Citation of meeting abstracts where part of this work was previously presented:

Kwok YN (1992) Effect of selective adenosine A1 and A2 analogs on the release of gastric somatostatin-like immunoreactivity. *Regul Pept* 40:189.

Kwok YN (1994) Purinergic control of release of somatostatin in the rat stomach. *Pathophysiology* Supplement 1:218.

Yip L and Kwok Y (2002) Gastric A1 and A2A receptors: cellular localization, gene sequence and gene expression levels. *Drug Dev Res* 56:551.

Yip L, Leung CH and Kwok YN (2003) Cellular localization of adenosine A1 and A2A receptors in the rat stomach. *FASEB J* 17:A40.

Please send reprints to: Yin Nam Kwok Ph.D., Department of Physiology, University of British Columbia, 2146 Health Sciences Mall, Vancouver, BC. Canada. V6T 1Z3. Tel: 604-822-6228, Fax: 604-822-6048, Email: kynkwok@interchange.ubc.ca

Figure Legends

Fig. 1 Effect of CPA, CGS 21680 and IB-MECA on gastric SLI release. Results are expressed as SLI release (%) as described in the Methods section. Each column represents the mean ± SEM of at least 5 experiments. *P < 0.05 when compared with period 3 using repeated measures ANOVA followed by Dunnett's multiple comparison test.

Fig. 2 Effect of various concentrations of adenosine agonists on gastric SLI release. The effect of CGS 21680 (■), CPA (●), CHA (×), S-PIA (□), R-PIA (△), IB-MECA (✸), 2-CA (◆) and NECA (○) were examined. Results are expressed as percentage (%) changes and calculated as described in the Methods section. Each point represents the mean ± SEM of at least 5 experiments.

Fig. 3 Effect of CGS 21680 and nitroprusside on perfusion pressure. Each column represents the mean ± SEM of at least 4 experiments; *P < 0.05 when compared to basal perfusion pressure. The inset shows a representative tracing of the effect of 1 μM nitroprusside on perfusion pressure.

Fig. 4 Effect of ZM 241385 on basal and stimulated SLI release. A: The effect of CGS 21680 (CGS) on basal SLI release; B: The effect of ZM 241385 on basal SLI release; C: The effect of ZM 241385 on CGS-stimulated release of SLI. Each column represents the mean ± SEM of at least 4 experiments; *P < 0.05 when compared with period 3 of respective experiments using repeated measures ANOVA followed by Dunnett's multiple comparison test.

Fig. 5 Effect of ZM 241385 and DPCPX on basal and CGS 21680 (CGS)- and adenosine-stimulated SLI release. Results are expressed as % changes, and each column represents the mean ± SEM of at least 4 experiments; $^{\dagger}P < 0.05$ and $^{\dagger\dagger}P < 0.01$ when comparing the mean SLI release (pg/min) in the presence of ZM 241385 or DPCPX during periods 4-7 with that of periods 1-3 (basal release), $^{**}P < 0.01$ when compared with the agonist-induced release of SLI.

Fig. 6 Effect of EHNA and ADA on basal (A) and adenosine (ADO)-induced (B) SLI release. Results are expressed as % changes of SLI release, and each column represents the mean ± SEM of at least 4 experiments. A: $^{*}P < 0.05$ and $^{**}P < 0.01$ when comparing the mean SLI release (pg/min) in the presence of EHNA or ADA during periods 4-7 with that of periods 1-3 (basal release). B: $^{*}P < 0.05$ and $^{**}P < 0.01$ when compared with ADO-induced release of SLI.

Fig. 7 Confocal images showing A_{2A}R-IR in the corpus and antrum of the rat stomach. A: A_{2A}R-IR cell in the corporeal mucosa. B: A_{2A}R-IR on nerves fibers and cell bodies of the myenteric plexus (arrowheads), and on nerve fibers of the circular (CM) and longitudinal (LM) muscle layers (arrows) of the corpus. C: A_{2A}R-IR on blood vessels (arrowheads) and nerve fibers (arrow) in the submucosal plexus (SMP) of the antrum. D: A_{2A}R-IR on nerve fibers and cell bodies of the myenteric plexus (arrowhead), and on nerve fibers of the circular and longitudinal muscle (arrows) of the antrum. Scale bars = 25 μm (z-step = 1.0 μm for all images).

Fig. 8 Confocal images showing the co-localization of A_{2A}R-IR with somatostatin-IR in the rat stomach. Cells expressing both A_{2A}R-IR and somatostatin-IR are indicated by arrows and appear yellow (C, F, I & L). A_{2A}R-IR is expressed on some somatostatin-IR cells of the corpus

(A-C) and antrum (D-F). Co-localization of A_{2A}R-IR with somatostatin-IR in the myenteric plexus was also observed, but occurred very infrequently. Co-localization of A_{2A}R-IR and somatostatin is shown in the myenteric plexus of the corpus (G-I) and antrum (J-L). LM = longitudinal muscle, CM = circular muscle. Scale bars = 25 μm. (z-step = 0.5 μm for all images).

Fig. 9 Double-staining of A_{2A}R-IR with H^+K^+-ATPase β, Gastrin, VWF, and PGP 9.5-IR in the rat stomach. Cells expressing both immunoreactivities appear yellow (I & L). A-C: A_{2A}R-IR (A) was shown not to co-localize with H^+K^+-ATPase β-IR (B) in the corpus mucosa (C). D-F: A_{2A}R-IR (D) was also shown not to co-localize with gastrin-IR (E) in the antral mucosa (F). G-I: A_{2A}R-IR (G) is co-localized with VWF-IR (H) on blood vessels in the myenteric region of the antrum (I). LM = longitudinal muscle, CM = circular muscle. J-L: A_{2A}R-IR (G) is co-localized with PGP 9.5 (H) in nerve fibers and cell bodies of the myenteric plexus (arrowhead), and nerve fibers of the circular and longitudinal muscle (arrows) of the corpus. Scale bars = 25 μm. (z-step = 1.0 μM for all images).

Fig. 10 Distribution and abundance of A_{2A} receptor mRNA in the rat stomach. A: RT-PCR was performed using primers which span the entire coding region of the A_{2A} receptor gene. A single amplicon was generated using cDNA from the fundus (lane 2), corpus (lane 3), antrum (lane 4) mucosa (lane 5) and striatum (positive control; lane 1) as the template. Ladder = 100 bp ladder. B: A_{2A} receptor gene expression levels measured in various regions of the rat stomach by quantitative Real-Time RT-PCR. Each bar represents the mean ± SEM of at least 4 animals; *P < 0.05 when compared to fundus, corpus, antrum and corporeal muscle using the unpaired

Student's t-test. C: A Real-Time RT-PCR standard curve generated using various amounts of A_{2A} receptor RNA as the template. Correlation coefficient = 0.98.

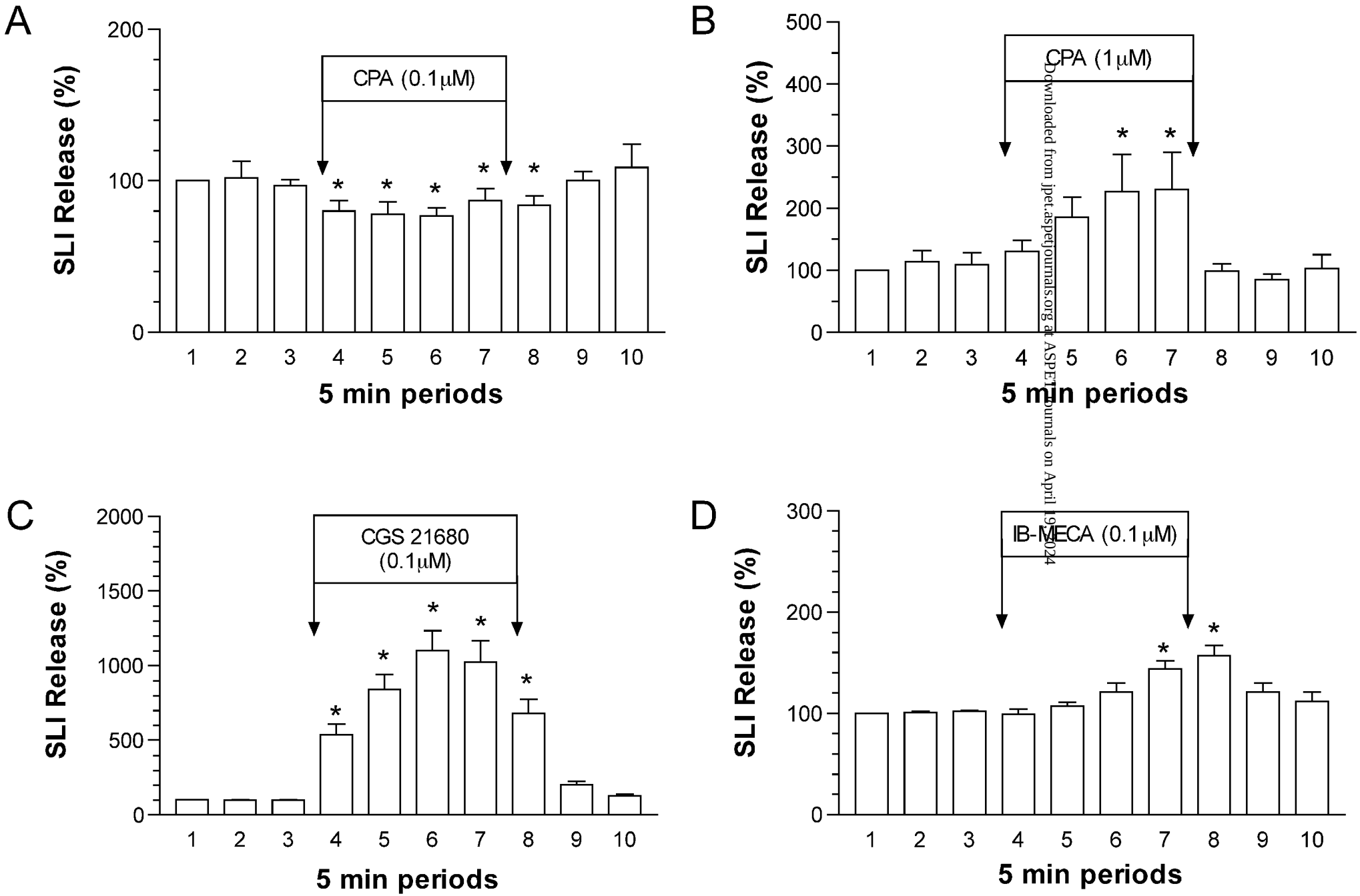

Fig. 1

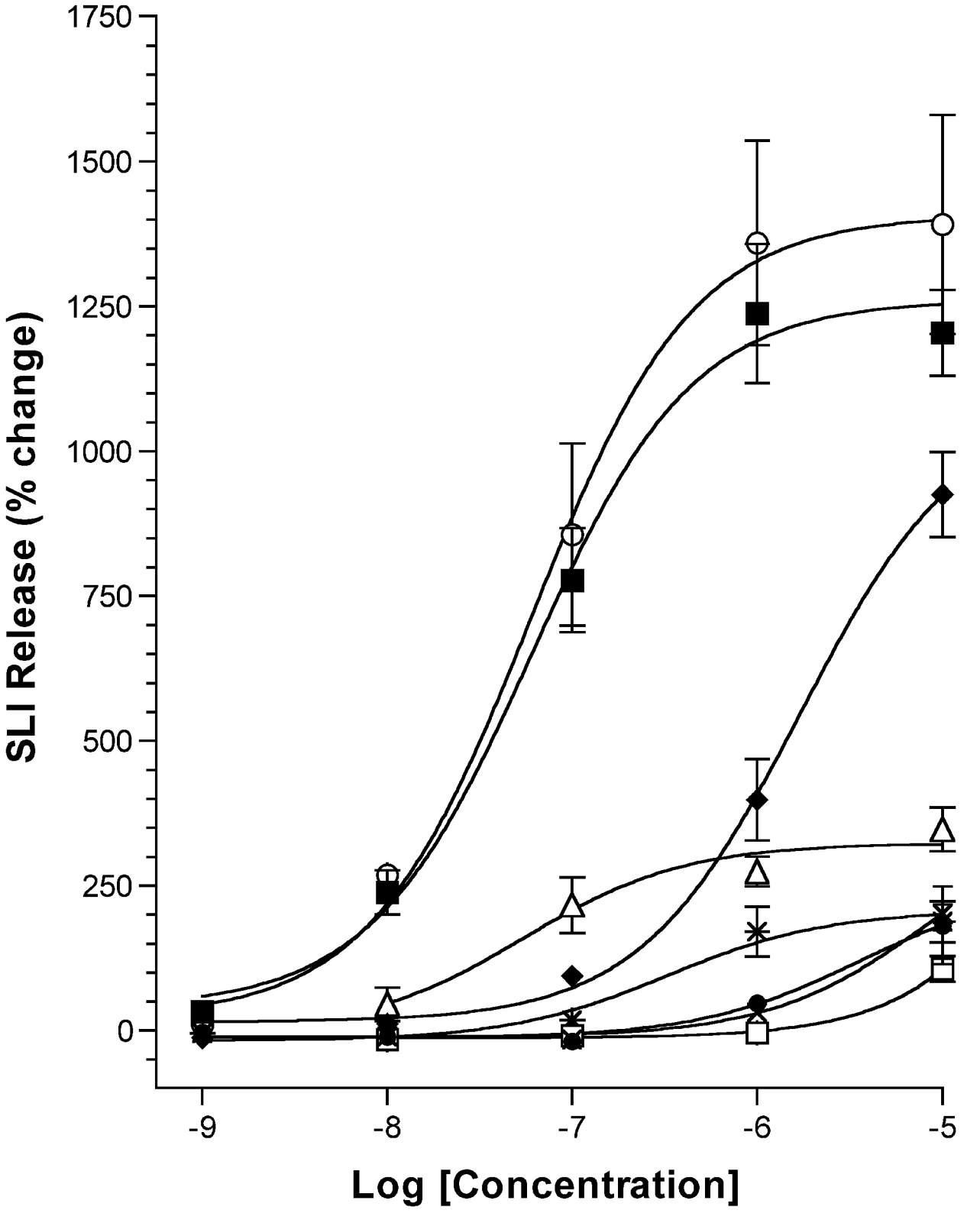
1750
1500
1250
1000
750
500
250
0
SLI Release (% change)
-9
-8
-7
-6
-5
Log [Concentration]

Fig. 2

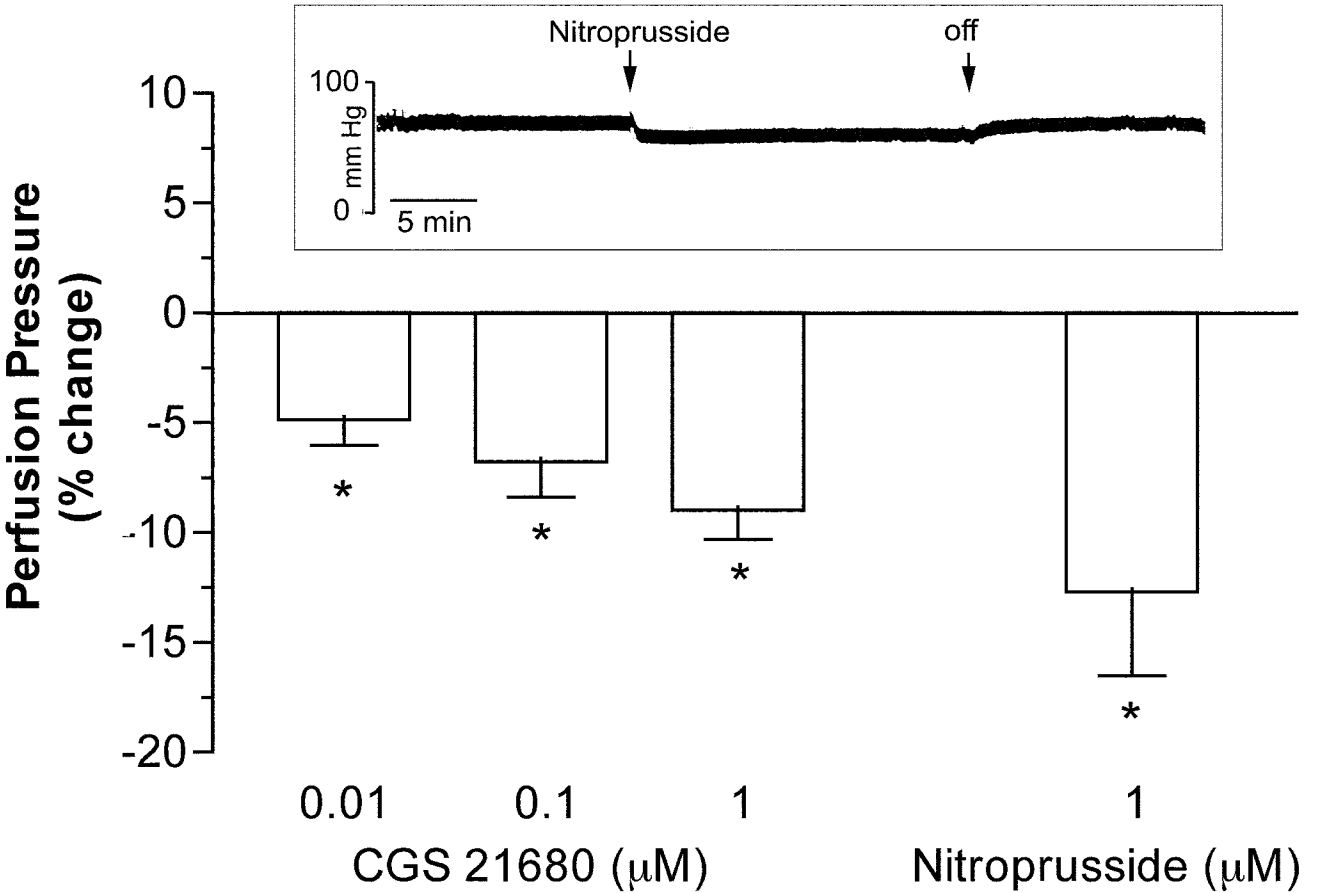
Nitroprusside
off
100
mm Hg
0
5 min
10
5
0
-5
-10
-15
-20
Perfusion Pressure
(% change)
*
*
*
*
0.01
0.1
1
1
CGS 21680 (μM)
Nitroprusside (μM)

Fig. 3

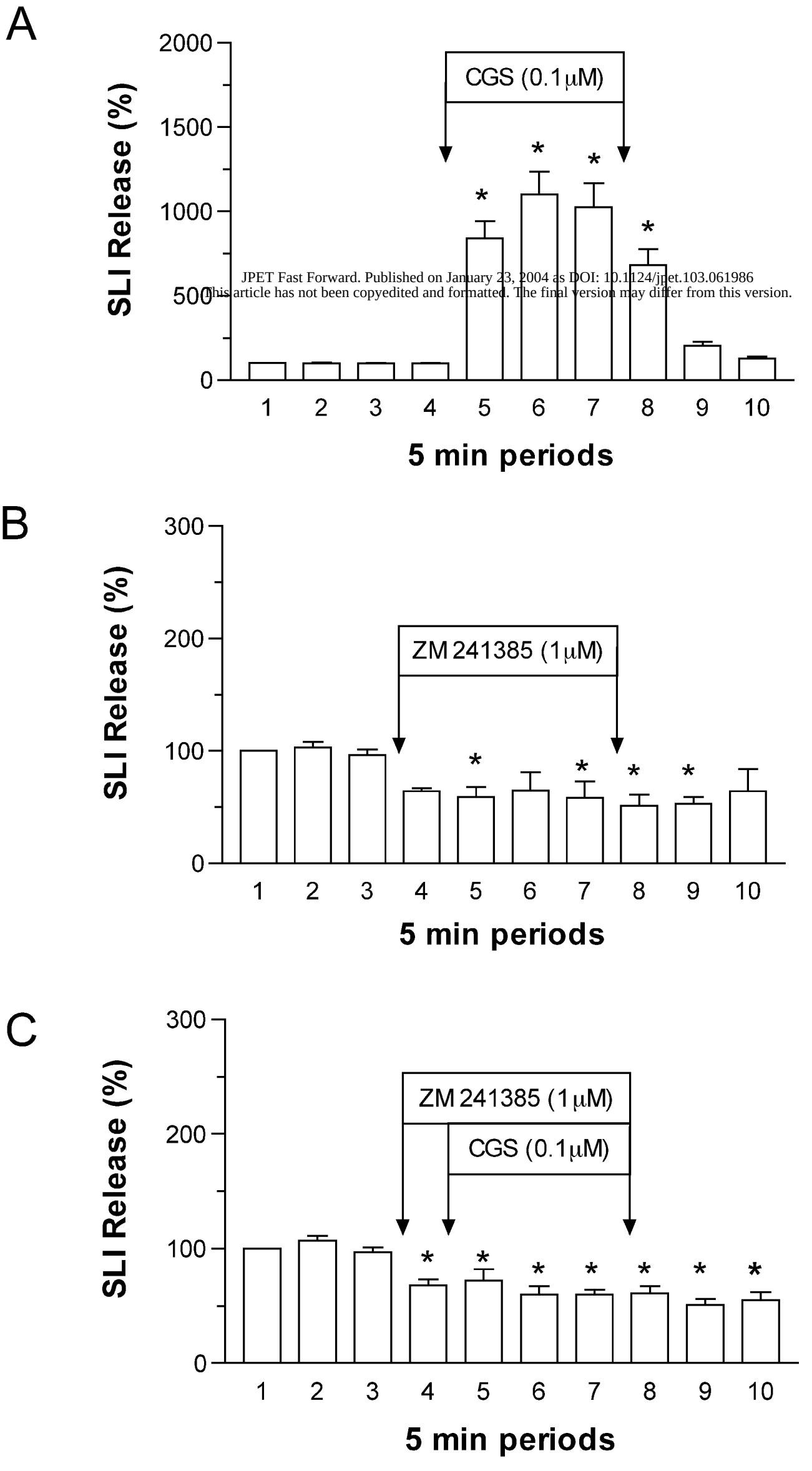

Fig. 4

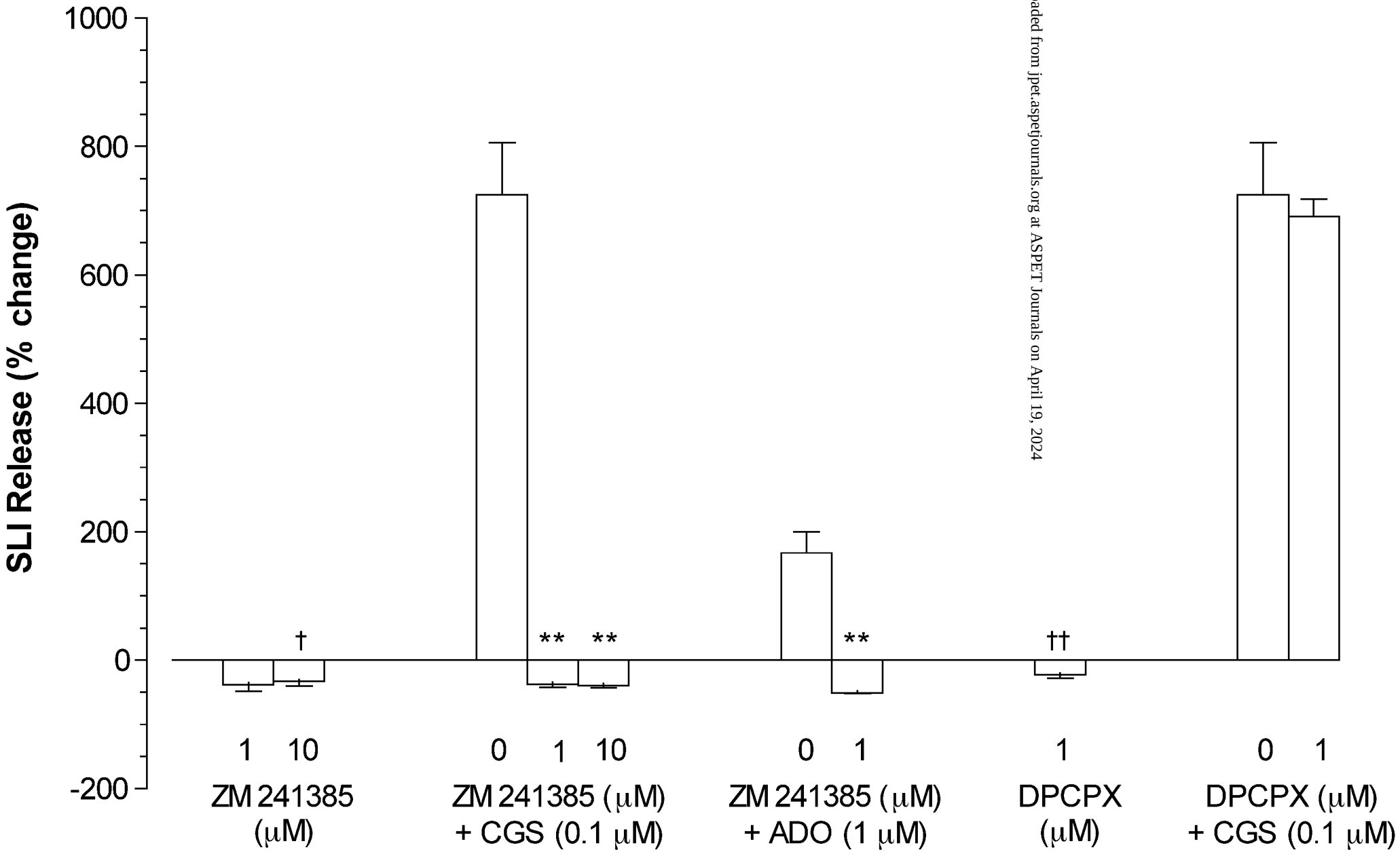

Fig. 5

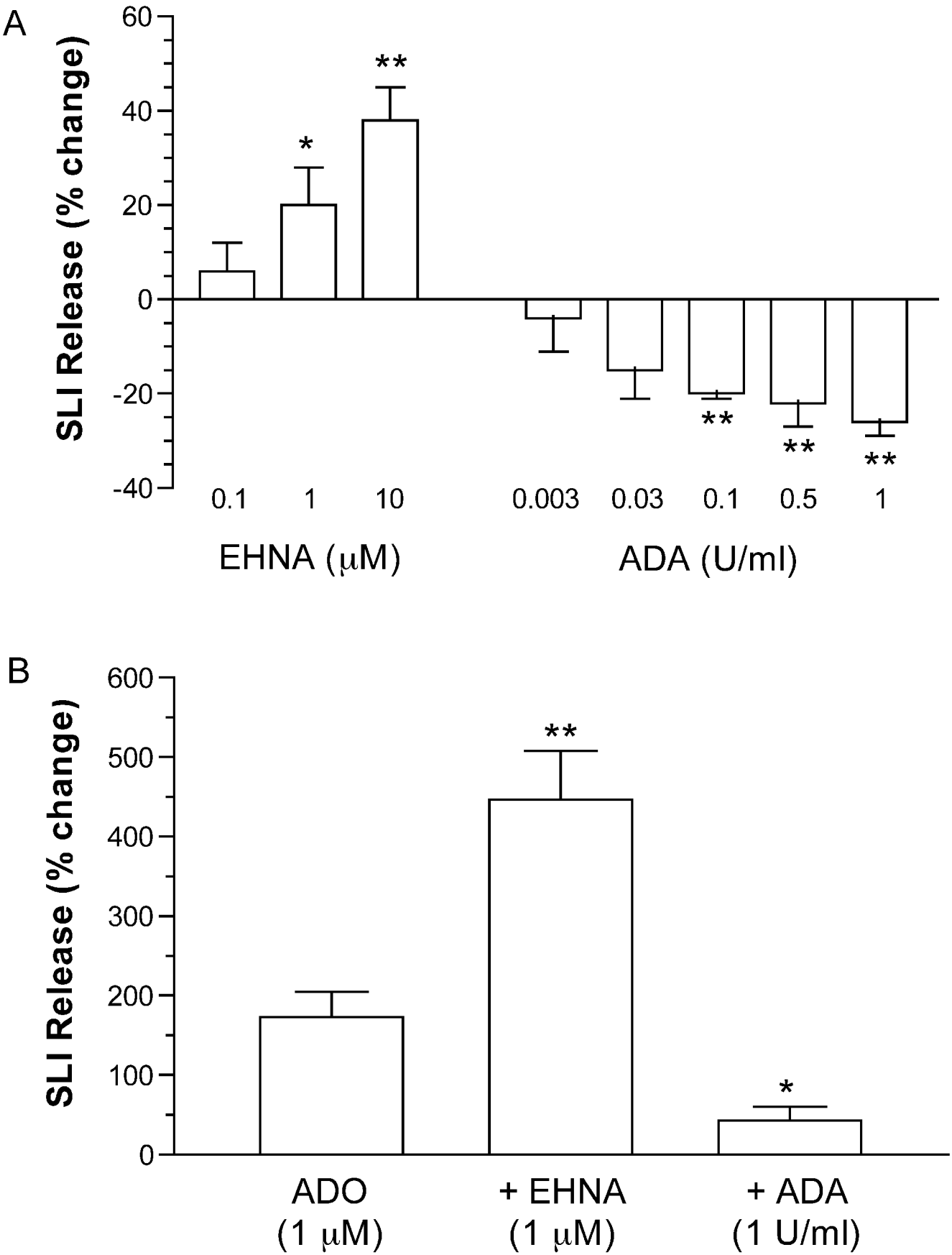
A
SLI Release (% change)
60
40
20
0
-20
-40
*
**
**
**
**
0.1
1
10
0.003
0.03
0.1
0.5
1
EHNA (μM)
ADA (U/ml)
B
SLI Release (% change)
600
500
400
300
200
100
0
**
*
ADO
(1 μM)
+ EHNA
(1 μM)
+ ADA
(1 U/ml)

Fig. 6

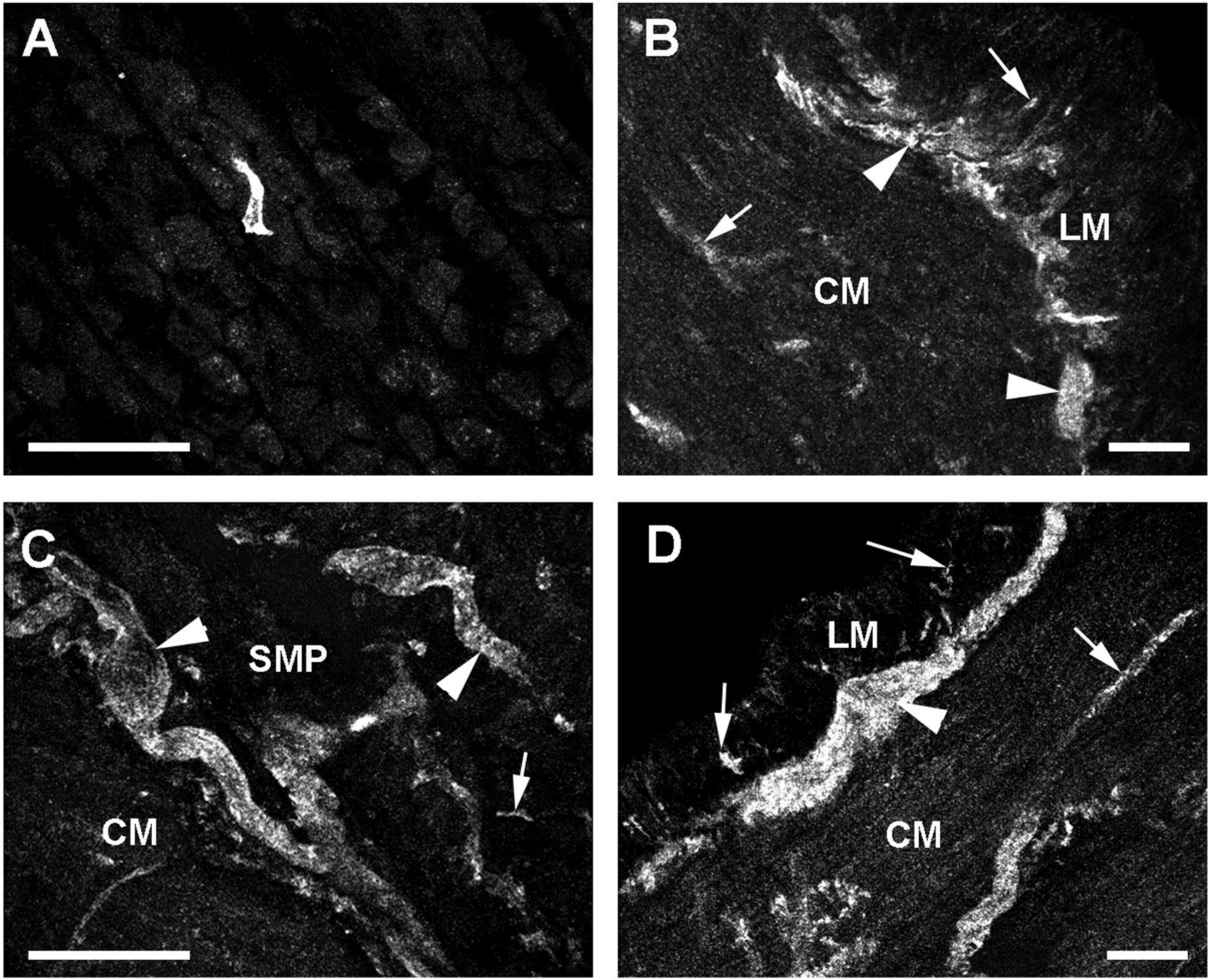

Fig. 7

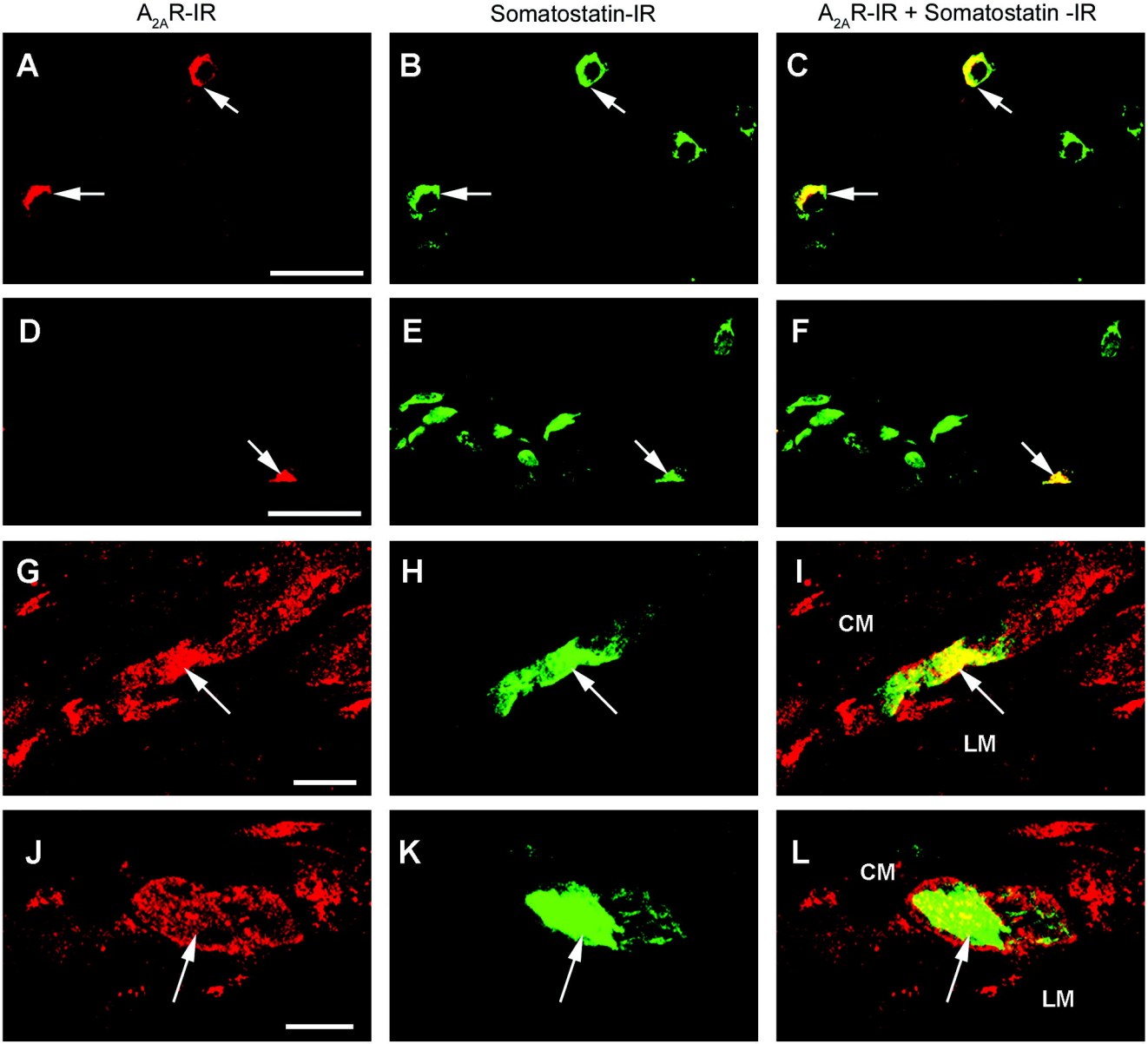
A2AR-IR
Somatostatin-IR
A2AR-IR + Somatostatin -IR
A
B
C
D
E
F
G
H
I
CM
LM
J
K
L
CM
LM

Fig. 8

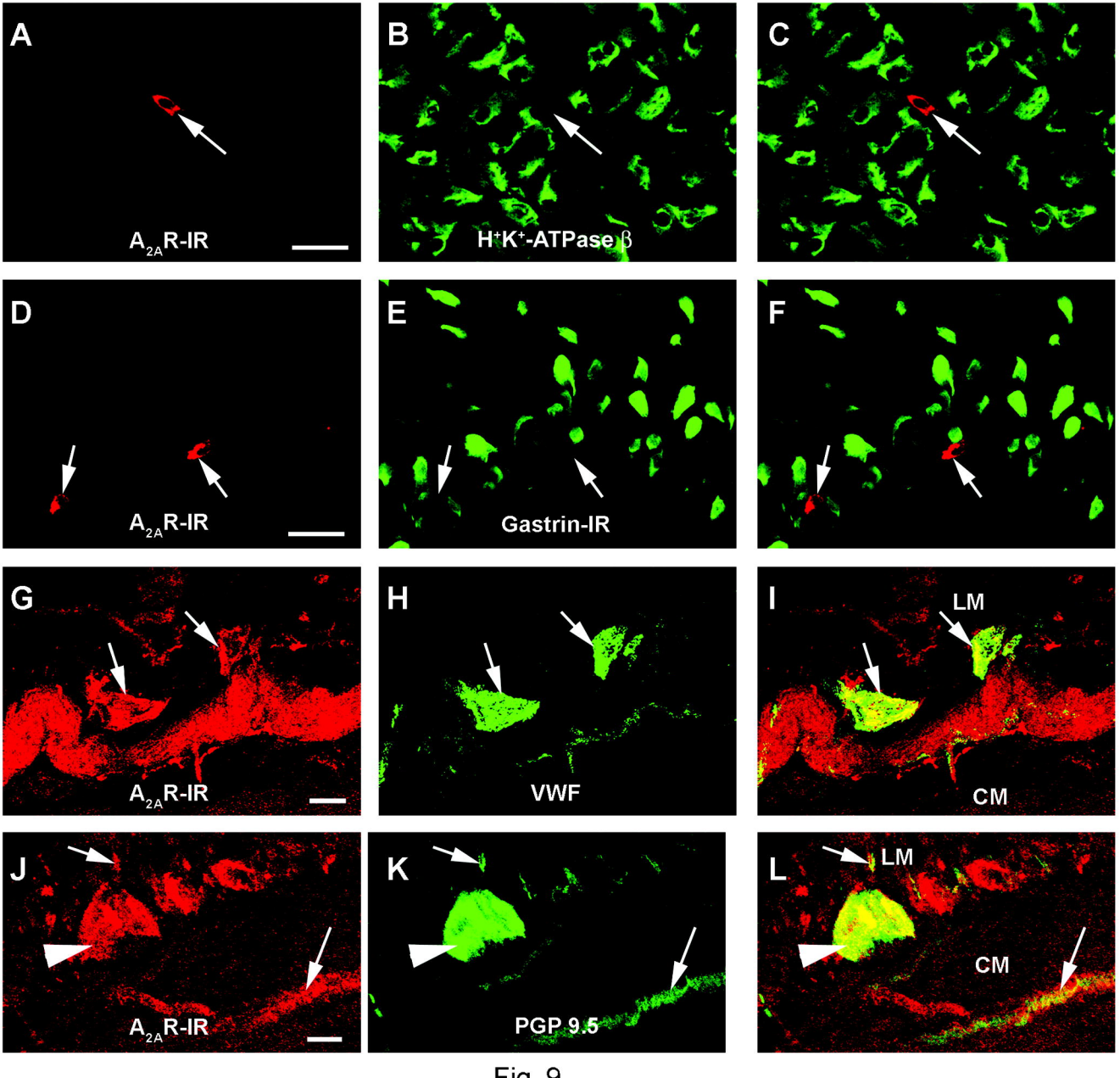
A
A2AR-IR
B
H+K+-ATPase β
C
D
A2AR-IR
E
Gastrin-IR
F
G
A2AR-IR
H
VWF
I
LM
CM
J
A2AR-IR
K
PGP 9.5
L
LM
CM

Fig. 9

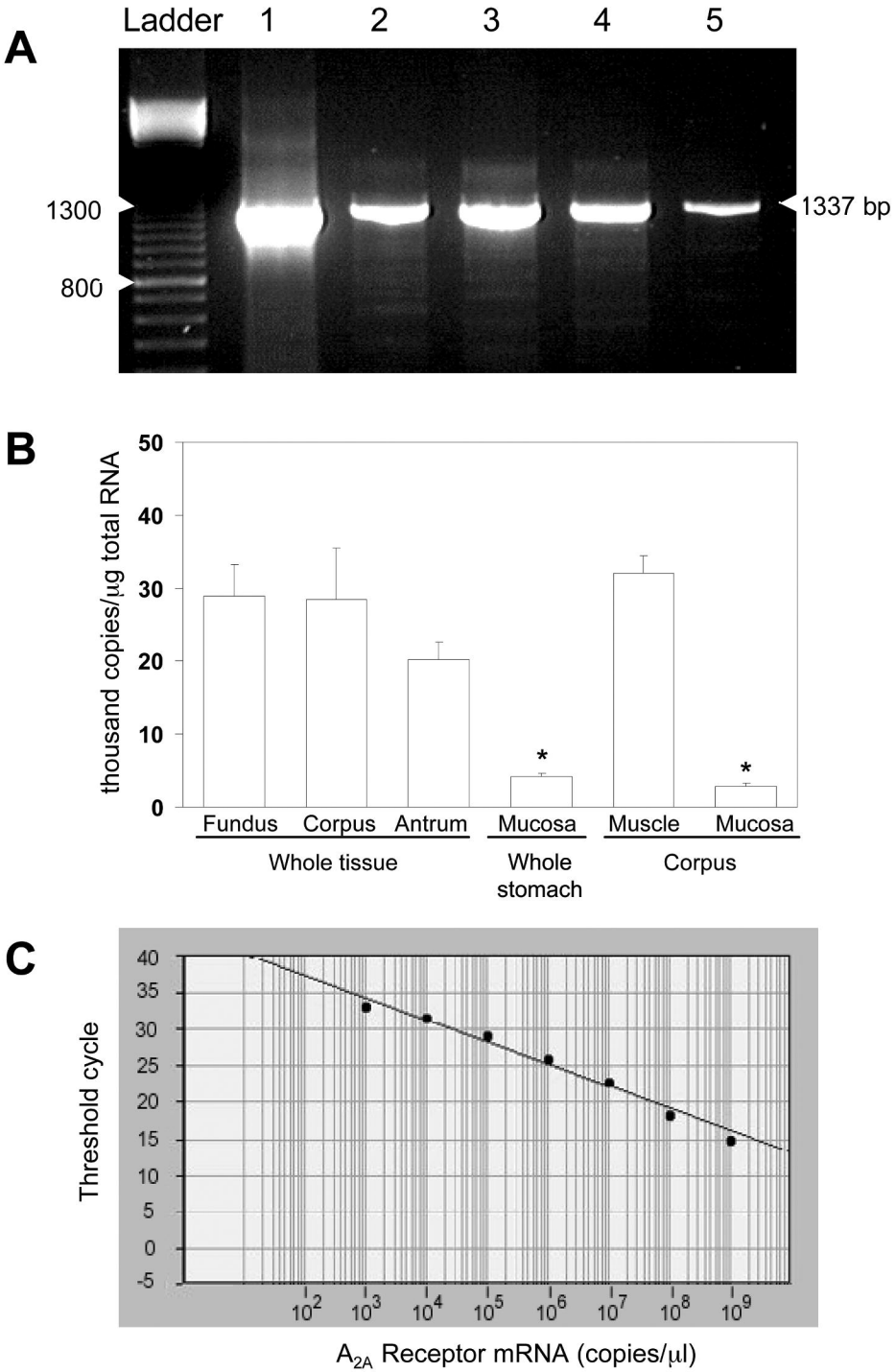
A
Ladder
1
2
3
4
5
1300
800
1337 bp
B
thousand copies/μg total RNA
50
40
30
20
10
0
*
*
Fundus
Corpus
Antrum
Mucosa
Muscle
Mucosa
Whole tissue
Whole stomach
Corpus
C
Threshold cycle
40
35
30
25
20
15
10
5
0
-5
10^2
10^3
10^4
10^5
10^6
10^7
10^8
10^9
A_{2A} Receptor mRNA (copies/μl)

Fig. 10